**Noname manuscript No.**
(will be inserted by the editor)

# A Laminate Parametrization Technique for Discrete Ply-Angle Problems with Manufacturing Constraints

**Graeme J. Kennedy · Joaquim R. R. A. Martins**

the date of receipt and acceptance should be inserted later

**Abstract** In this paper we present a novel laminate parametrization technique for layered composite structures that can handle problems in which the ply angles are limited to a discrete set. In the proposed technique, the classical laminate stiffnesses are expressed as a linear combination of the discrete options and design-variable weights. An exact $\ell_1$ penalty function is employed to drive the solution toward discrete 0–1 designs. The proposed technique can be used as either an alternative or an enhancement to SIMP-type methods such as discrete material optimization (DMO). Unlike mixed-integer approaches, our laminate parametrization technique is well suited for gradient-based design optimization. The proposed laminate parametrization is demonstrated on the compliance design of laminated plates and the buckling design of a laminated stiffened panel. The results demonstrate that the approach is an effective alternative to DMO methods.

## 1 Introduction

The parametrization of laminated composite structures for design optimization is a challenging problem. Often, due to manufacturing limitations, the allowable ply angles are restricted to a discrete set of values. This discrete problem is not, in its most natural form, amenable to gradient-based optimization. On the other hand, methods for nonlinear mixed-integer programming are almost inevitably computationally expensive, especially for large design spaces. Here, we present a laminate parametrization that takes into account the discrete nature of the ply angles. To avoid solving a large nonlinear, mixed-integer program, we use a relaxation approach where the original discrete problem is transformed into a continuous

This work was previously presented by the authors under the title "A regularized discrete laminate parametrization technique with applications to wing-box design optimization" at the 53rd AIAA/ASME/ASCE/AHS/ASC Structures, Structural Dynamics, and Materials Conference, Honolulu, HI, April 2012.

G.J. Kennedy
University of Michigan, Department of Aerospace Engineering, Ann Arbor, MI, USA
E-mail: graeme.j.kennedy@gmail.com

J.R.R.A. Martins
University of Michigan, Department of Aerospace Engineering, Ann Arbor, MI, USA
E-mail: jrram@umich.edu

analog of the original problem. We then obtain solutions to the modified problem using gradient-based optimization.

Many different authors have developed laminate parametrization techniques. These techniques generally fall into two categories: direct parametrizations that provide an explicit description of the physical laminate, and indirect parametrizations in which intermediate variables are employed and the lamination sequence is available only in a post-processing calculation. There are difficulties with both of these approaches. Direct techniques often introduce many local minima in the design space, while indirect methods make it difficult to impose manufacturing constraints on the physical construction of the laminate. Here we use a direct parametrization of the laminate and accept the possibility of local minima; this approach allows us to impose manufacturing requirements on the lamination sequence.

The remainder of the paper is structured as follows. In Section 2 we review the relevant literature on laminate parametrization techniques, and in Section 3 we describe our proposed technique. In Section 4 we describe additional manufacturing constraints that may be required for certain laminate design problems. In Section 5 we present the results from two compliance minimization studies, verifying our approach against previous work and demonstrating the approach in a novel application. In Section 6 we present the results from a series of buckling design problems that incorporate important manufacturing constraints.

## 2 Literature review

The use of ply-angle variables and the integer number of plies is the most direct parametrization of a lamination sequence. However, this type of parametrization suffers from several drawbacks. First, it necessitates mixed-integer programming techniques [Haftka and Gürdal, 1992]. Second, it is well known that the parametrization using ply-angle variables, for a fixed number of plies, introduces many local minima [Stegmann and Lund, 2005]. Authors have developed various techniques to address these issues. For instance, Bruyneel and Fleury [2002] and Bruyneel [2006] developed an effective gradient-based optimization approach for composite structures parametrized with ply angles, for stiffness, strength, and weight design criteria. Despite these successful applications, these parametrizations cannot directly address manufacturing constraints that limit the available ply angles to a discrete set.

Another common technique is to use the lamination parameters first introduced by Tsai and Pagano [1968]. In this approach, the constitutive matrices in classical lamination theory (CLT) or in first-order shear deformation theory (FSDT) are expressed in terms of the material invariants and the lamination parameters, which are twelve integrals of trigonometric functions of the ply-angle distribution through the thickness of the laminate. Because of the relationship between these integrals, not all combinations of the lamination parameters represent physically realizable laminates. As a result, constraints must be imposed to restrict the values of the parameters to a physically realizable domain [Hammer et al., 1997]. An expression for the full feasible space of lamination parameters is not known explicitly, so often a subset of the variables is used for the design.

Lamination parameters have often been used as a parametrization for stiffness and buckling design. Fukunaga and Vanderplaats [1991] performed a buckling optimization of cylindrical shells with symmetric orthotropic laminates using two in-plane and two flexural lamination parameters. They also solved the inverse problem to obtain the explicit lamination sequences. Later, Fukunaga and Sekine [1992] performed a stiffness design of laminates and obtained explicit expressions for the feasible space of symmetric laminates. Miki and Sugiyama [1993] used lamination parameters for the compliance and buckling design of

symmetric orthotropic laminates. Hammer et al. [1997] presented an extensive theoretical development of the mathematical properties of lamination parameters and used them for the compliance design of symmetric laminates subject to single and multiple loading conditions. Liu et al. [2004] designed simply supported symmetric plates for buckling using lamination parameters. They imposed constraints on the number of plies at $0^o$, $\pm 45^o$, and $90^o$ and mapped these constraints into a hexagonal region in the lamination parameter space.

Other authors have extended the use of the lamination parameters beyond stiffness and buckling design applications. Foldager et al. [1998] used lamination parameters to avoid local minima while performing compliance minimization using ply-angle design variables. IJsselmuiden et al. [2008] performed strength-based design studies using lamination parameters by incorporating the Tsai–Wu failure criteria [Jones, 1996] into the lamination parameter space to obtain a conservative failure envelope.

While lamination-parameter-based techniques have been used effectively in many applications, one of the primary disadvantages of these approaches is that they do not provide a direct description of the laminate construction. This makes it difficult to impose the constraints on the ply angles that may be required by manufacturing considerations. Furthermore, lamination parameters by themselves do not provide a lamination sequence and therefore can be viewed only as an intermediate design result.

Often, for manufacturing reasons, the ply angles available to the designer are restricted to a discrete set of options such as $0^o$, $\pm 45^o$, and $90^o$. With this restriction, the laminate sequence design problem becomes a mixed-integer programming problem. Various authors have used either mixed-integer programming techniques or genetic algorithms (GAs) to solve laminate stacking sequence problems with a discrete set of ply angles. Haftka and Walsh [1992] formulated a buckling-load maximization of a simply supported plate, with and without ply-contiguity constraints, as a linear integer programming problem and obtained globally optimal designs using a branch and bound algorithm. Le Riche and Haftka [1993] used a GA to perform a buckling-load maximization of a simply supported plate with strength and ply-contiguity constraints. Later, Liu et al. [2000] used a permutation GA to perform a buckling-load maximization for a simply supported plate with a constraint on the number of plies at each available angle. Adams et al. [2004] used a GA for a realistic composite wing-box design problem with a thick guide laminate and blended plies.

The main advantage of using GAs for laminate design problems is that they have the ability to work directly with integer variables. Furthermore, GAs may obtain the global optimum, regardless of whether the underlying design space is multimodal or discontinuous. However, GAs usually require many more function evaluations than gradient-based approaches do, especially for large design spaces. This property of GAs is especially problematic when employing high-fidelity computational methods that require significant computational time for a single analysis.

Discrete material optimization (DMO) approaches can be used as either multimaterial parametrizations or as direct laminate sequence parametrizations. DMO was first proposed by Stegmann and Lund [2005] as a generalization of the approach of Sigmund and Torquato [1997]. When the DMO approach is applied to laminate design, the stiffness contribution from every discrete ply angle in each layer is multiplied by a weighting function. Instead of a linear interpolant, a SIMP-type penalization is employed such that the stiffness-to-weight ratios of the intermediate designs are less favorable. Stegmann and Lund [2005] and later Lund [2009] applied the DMO approach to compliance and buckling optimization for composite shells.

Other authors have extended the SIMP and DMO approaches. Bruyneel [2011] developed an approach similar to DMO for selection from a discrete set of four plies via bilinear

shape function weights. This approach, called the shape function with penalization (SFP) parametrization, reduces the number of design variables compared to DMO approaches. Bruyneel et al. [2011] extended the SFP approach to material selection from different numbers of plies by using different interpolation functions. Recently, Gao et al. [2012] developed a bi-value coding parameterization (BCP) that extends the SFP approach and is particularly well suited for problems with large numbers of discrete ply angles or candidate materials. Using a different approach, Hvejsel et al. [2011] developed a technique for laminate parametrization that, in a similar manner to DMO, uses a weighted sum of contributions to the stiffness. In a departure from the DMO approach, they employed an exact quadratic concave penalty constraint function, first used by Borrvall and Petersson [2001], to force the design toward a discrete solution. They demonstrated their approach on a series of compliance minimization problems. Hvejsel and Lund [2011] extended the SIMP interpolation scheme to multimaterial selection problems, including ply-angle selection. In a departure from DMO-type methods, many sparse linear constraints are required within the parametrization.

One of the main advantages of DMO and DMO-type parametrizations is that they can be used with gradient-based optimization techniques. As a result, DMO parametrizations can be used on very large problems that might not otherwise be amenable to gradient-free methods such as GAs. However, DMO approaches may produce only a locally optimal solution. Furthermore, DMO and DMO-type approaches may fail to converge to a fully discrete design, especially for objectives other than compliance, and it may be difficult to assess the merits of an intermediate solution.

In this paper, we present a direct laminate parametrization technique that is a continuous regularization of a discrete mixed-integer laminate formulation. Similarly to the DMO approach of Stegmann and Lund [2005], we interpolate between a discrete set of possible angles using a linear combination of material stiffnesses. In a departure from previous work, we add an exact $\ell_1$ penalty function to the objective to force the design toward a discrete solution. The $\ell_1$ penalty function is not differentiable, so we use an elastic programming approach that produces the effect of the $\ell_1$ norm in a differentiable manner within the optimization problem. We show that simplifications to the penalization can be made if certain linear constraints are satisfied exactly at all optimization iterations. We demonstrate, with numerical examples, that this penalization is very effective for both compliance and buckling design optimization problems. In a departure from previous papers on DMO-type methods, we introduce additional constraints on the ply angles that may arise from manufacturing considerations. These constraints are imposed using a complementarity constraint formulation handled through a regularization technique proposed by Scheel and Scholtes [2000] and Scholtes [2001].

## 3 The proposed laminate parametrization

In the following laminate parametrization technique, we consider a structure that is split into a series of $M$ design segments. Each design segment is composed of a single laminate with $N$ layers, where in each layer the ply angles must be selected from a discrete set of $K$ allowable angles, $\Theta = \{\theta_1, \theta_2, \ldots, \theta_K\}$. For ease of presentation, we have fixed the number of layers and the number of allowable ply angles to $N$ and $K$ for all segments. This restriction is not required, and in general the number of plies and number of available ply angles may vary between design segments.

Each design segment of the structure is modeled using an FSDT approach, where the in-plane, bending-stretching coupling, bending, and transverse shear constitutive matrices are: $\mathbf{A}^{(i)}$, $\mathbf{B}^{(i)}$, $\mathbf{D}^{(i)}$, $\mathbf{A}_s^{(i)}$. Here the superscript $i$ indexes the $i^{\text{th}}$ design segment, where $i = 1,\ldots,M$.

In the following description, we first outline the proposed laminate parametrization using a mixed-integer formulation. We then proceed to relax the discrete problem to a continuous formulation. In the proposed technique, we express the constitutive matrices, $\mathbf{A}^{(i)}$, $\mathbf{B}^{(i)}$, $\mathbf{D}^{(i)}$, and $\mathbf{A}_s^{(i)}$, in terms of a series of discrete ply-identity variables $\xi_{ijk} \in \{0, 1\}$:

$$\begin{aligned}
\mathbf{A}^{(i)} &= \sum_{j=1}^{N} (h_{ij+1} - h_{ij}) \sum_{k=1}^{K} \xi_{ijk} \bar{\mathbf{Q}}(\theta_k), \\
\mathbf{B}^{(i)} &= \sum_{j=1}^{N} \frac{1}{2} (h_{ij+1}^2 - h_{ij}^2) \sum_{k=1}^{K} \xi_{ijk} \bar{\mathbf{Q}}(\theta_k), \\
\mathbf{D}^{(i)} &= \sum_{j=1}^{N} \frac{1}{3} (h_{ij+1}^3 - h_{ij}^3) \sum_{k=1}^{K} \xi_{ijk} \bar{\mathbf{Q}}(\theta_k), \\
\mathbf{A_s}^{(i)} &= \kappa \sum_{j=1}^{N} (h_{ij+1} - h_{ij}) \sum_{k=1}^{K} \xi_{ijk} \bar{\mathbf{Q}}_s(\theta_k),
\end{aligned} \tag{1}$$

where there are $N$ plies in the laminate, $\bar{\mathbf{Q}}(\theta)$ and $\bar{\mathbf{Q}}_s(\theta)$ are the laminae in-plane and shear stiffnesses in the global coordinate system [Jones, 1996], and $h_{ij}$ is the through-thickness coordinate of the $j^{\text{th}}$ layer-interface in the $i^{\text{th}}$ design segment.

An active ply-identity variable, $\xi_{ijk} = 1$, indicates that the $k^{\text{th}}$ ply angle, $\theta_k$, in the $j^{\text{th}}$ layer of the $i^{\text{th}}$ design segment has been selected. To avoid selecting multiple ply angles in the same layer, we impose the following constraint:

$$\sum_{k=1}^{K} \xi_{ijk} = 1, \quad i = 1,\ldots,N, \quad j = 1,\ldots,M. \tag{2}$$

This discrete formulation is equivalent to the linear mixed-integer approach of Haftka and Walsh [1992]. Equation (2) ensures that one and only one ply is active in each layer, i.e., $\xi_{ijp} = 1$ for some $p$, while $\xi_{ijk} = 0$ for $k \neq p$.

The number of possible designs increases rapidly as the numbers of ply angles, layers, and design segments increase. Evaluating all possible designs quickly becomes computationally intractable since there are $K^{MN}$ possible combinations.

Instead of using the discrete variables $\xi_{ijk} \in \{0, 1\}$, we relax the mixed-integer problem and use continuous variables: $x_{ijk} \in [0, 1]$. We refer to these variables as ply-selection variables and refer to continuous designs that satisfy $x_{ijk} \in \{0, 1\}$ as 0–1 solutions. The stiffness can now be expressed in terms of the continuous ply-selection variables as follows:

$$\begin{aligned}
\mathbf{A}^{(i)} &= \sum_{j=1}^{N} (h_{ij+1} - h_{ij}) \sum_{k=1}^{K} x_{ijk}^P \bar{\mathbf{Q}}(\theta_k), \\
\mathbf{B}^{(i)} &= \sum_{j=1}^{N} \frac{1}{2} (h_{ij+1}^2 - h_{ij}^2) \sum_{k=1}^{K} x_{ijk}^P \bar{\mathbf{Q}}(\theta_k), \\
\mathbf{D}^{(i)} &= \sum_{j=1}^{N} \frac{1}{3} (h_{ij+1}^3 - h_{ij}^3) \sum_{k=1}^{K} x_{ijk}^P \bar{\mathbf{Q}}(\theta_k), \\
\mathbf{A_s}^{(i)} &= \kappa \sum_{j=1}^{N} (h_{ij+1} - h_{ij}) \sum_{k=1}^{K} x_{ijk}^P \bar{\mathbf{Q}}_s(\theta_k),
\end{aligned} \tag{3}$$

where $x_{ijk}$ are continuous over the interval $[0, 1]$. Note that we have introduced a SIMP penalty parameter $P$ as an exponent on the continuous ply-identity variables, and as a result this formulation is equivalent to the multimaterial formulation of Hvejsel and Lund [2011]. The purpose of the parameter $P$ is to penalize the stiffness of intermediate designs such that 0–1 points have more favorable stiffness-to-weight ratios. Often, a continuation approach is employed where a series of optimization problems is solved for increasing values of $P$ [James et al., 2009, 2008]. However, a 0–1 solution is not guaranteed in general when using SIMP penalization, even for large values of the parameter $P$ [Stolpe and Svanberg, 2001b,a]. To demonstrate that the proposed parametrization is effective without additional SIMP penalization, we set the parameter $P = 1$ for all the results presented in this paper. However, it must be emphasized that setting $P > 1$ would not affect the following development.

As in the mixed-integer formulation, we impose the following constraint on the continuous ply-angle selection variables:

$$\sum_{k=1}^{K} x_{ijk} = 1, \quad i = 1,\ldots,M, \quad j = 1,\ldots,N. \tag{4}$$

This constraint ensures that the weights are a partition of unity and that the design variables may be used to obtain a reasonable interpolation of the material properties. In the discrete case, this constraint is sufficient to ensure that a single material is active. However, in the continuous case, this constraint forces the design variables only to remain on a plane intersecting the coordinate axes at unity.

In the design problem, we collect all the design variables into the vector $\mathbf{x} \in \mathbb{R}^{MNK}$. We also collect all the linear constraints (4) for each design patch and each layer into the following expression:

$$\mathbf{A}_w \mathbf{x} = \mathbf{e}, \tag{5}$$

where $\mathbf{A}_w \in \mathbb{R}^{MN \times MNK}$ is a matrix and all the entries in the vector $\mathbf{e} \in \mathbb{R}^{MN}$ are 1.

In the proposed approach, we augment the SIMP penalization with an exact penalization technique. To force the design toward a 0–1 solution, we introduce the following constraint:

$$\sum_{k=1}^{K} x_{ijk}^2 = 1, \quad i = 1,\ldots,M, \quad j = 1,\ldots,N. \tag{6}$$

The conditions that the design variables are in the interval $[0, 1]$, sum to unity, and are on the unit $(K-1)$-sphere are sufficient to ensure that only one ply-selection variable, $x_{ijk}$, is active in each layer. In fact, the upper limit on the design variables $x_{ijk}$ is redundant and may be dropped. These criteria are shown graphically in Fig. 1, for $K = 3$, as the intersection of a 2-sphere and a plane for $x_1, x_2, x_3 \geq 0$.

For ease of presentation, the spherical constraints for all layers in all design segments are collected into a single vector constraint as follows:

$$\mathbf{c}_s(\mathbf{x}) - \mathbf{e} = 0, \tag{7}$$

where $\mathbf{c}_s(\mathbf{x}) \in \mathbb{R}^{MN}$ and $\mathbf{e} \in \mathbb{R}^{MN}$.

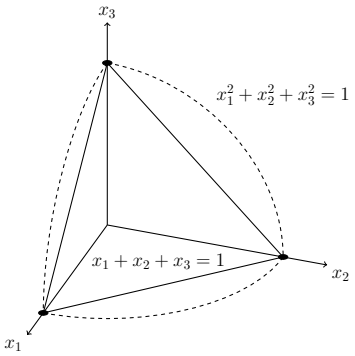


Fig. 1: Illustration of the spherical constraint, forcing the selection of a single ply-angle variable for each layer. This generalizes to arbitrary dimensions beyond $K = 3$.

If the objective of interest is $f(\mathbf{x})$, and any additional design constraints are written as $\mathbf{h}(\mathbf{x}) \geq 0$, the design optimization problem with the constraints (5) and (7) is:

$$\begin{aligned} \text{minimize} \quad & f(\mathbf{x}) \\ \text{w.r.t.} \quad & \mathbf{x} \geq 0 \\ \text{s.t.} \quad & \mathbf{h}(\mathbf{x}) \geq 0 \\ & \mathbf{c}_s(\mathbf{x}) - \mathbf{e} = 0 \\ & \mathbf{A}_w \mathbf{x} - \mathbf{e} = 0 \end{aligned} \tag{8}$$

The difficulty with this problem is that the spherical constraints (7) are highly nonlinear and introduce many local minima. To control this effect, we introduce the spherical constraint (7) through an exact $\ell_1$ penalty function with penalty parameter $\gamma$. The objective of this modified problem is $f(\mathbf{x}) + \gamma ||\mathbf{c}_s(\mathbf{x}) - \mathbf{e}||_1$ where $||\cdot||_1$ is the $\ell_1$ norm. However, this modified objective is not differentiable. Instead, we use an elastic programming technique [Nocedal and Wright, 1999] that creates the effect of the $\ell_1$ norm in a differentiable manner by adding additional slack variables to the optimization problem. Using the elastic programming approach, we introduce the vectors of slack variables $\mathbf{s}_+, \mathbf{s}_- \in \mathbb{R}^{MN}$ such that

$$\mathbf{c}_s(\mathbf{x}) - \mathbf{e} = \mathbf{s}_+ - \mathbf{s}_-, \tag{9}$$

where we impose $\mathbf{s}_+, \mathbf{s}_- \geq 0$. The slack variables $\mathbf{s}_+$ and $\mathbf{s}_-$ represent the positive and negative constraint violation of Eq. (7).

The modified optimization problem becomes:

$$\begin{aligned} \text{minimize} \quad & f(\mathbf{x}) + \gamma \mathbf{e}^T (\mathbf{s}_+ + \mathbf{s}_-) \\ \text{w.r.t.} \quad & \mathbf{x}, \mathbf{s}_+, \mathbf{s}_- \geq 0 \\ \text{s.t.} \quad & \mathbf{h}(\mathbf{x}) \geq 0 \\ & \mathbf{c}_s(\mathbf{x}) - \mathbf{e} = \mathbf{s}_+ - \mathbf{s}_- \\ & \mathbf{A}_w \mathbf{x} - \mathbf{e} = 0 \end{aligned} \tag{10}$$

where the parameter $\gamma > 0$ is a penalty parameter. For a feasible problem, with a sufficiently large but finite value of $\gamma$, Problem (10) admits solutions, $\mathbf{x}^*$, $\mathbf{s}_+^* = \mathbf{s}_-^* = 0$, that are also

solutions to Problem (8). However, as $\gamma \to 0$, Problem (10) admits solutions that are not solutions to Problem (8) and do not satisfy the 0–1 criterion. Our approach will be to solve the $\ell_1$ penalized optimization problem (10) for increasing values of the penalty parameter. For small $\gamma$, this will allow greater freedom in exploring the design space, and with increasing $\gamma$ the solution will tend toward a local minima with intermediate design-variable values or a 0–1 solution. As with DMO and other direct laminate parametrizations, the proposed approach can guarantee convergence only to a local minimum.

A further simplification of Problem (10) can be achieved when the summation constraints (5) are satisfied exactly at every iteration. Starting from Eq. (5), the sum of the squared design variables must be less than or equal to one, i.e.,

$$1 = \left( \sum_{k=1}^{K} x_{ijk} \right)^2 \geq \sum_{k=1}^{K} x_{ijk}^2.$$

As a result, when the linear constraint (5) is satisfied exactly, the constraint violation of Eq. (7) is negative, i.e., $\mathbf{c}_s(\mathbf{x}) - \mathbf{e} \leq 0$. Therefore, the values of the slacks at the solution are:

$$\begin{aligned} \mathbf{s}_+^* &= 0, \\ \mathbf{s}_-^* &= \mathbf{e} - \mathbf{c}_s(\mathbf{x}^*). \end{aligned}$$

This result can also be observed geometrically. Whenever the design lies on the plane, the distance from the origin to the sphere is always greater than the distance from the origin to the plane, unless the design is at a 0–1 point when the difference is precisely zero; see Fig. 1. Using this result, the optimization problem Opt($\gamma$) can be written as follows:

$$\begin{aligned} \text{minimize} \quad & f(\mathbf{x}) + \gamma \mathbf{e}^T (\mathbf{e} - \mathbf{c}_s(\mathbf{x})) \\ \text{w.r.t.} \quad & \mathbf{x} \geq 0 \\ \text{s.t.} \quad & \mathbf{h}(\mathbf{x}) \geq 0 \\ & \mathbf{A}_w \mathbf{x} \equiv \mathbf{e} \end{aligned} \tag{11}$$

where the final constraint is written as $\mathbf{A}_w \mathbf{x} \equiv \mathbf{e}$ to indicate that it is satisfied at every iteration.

We use a continuation approach and solve Opt($\gamma_n$) for a sequence of increasing $\gamma_n$, starting each subsequent optimization problem from the previous solution. We terminate the sequence once the design satisfies the 0–1 criterion. For all design problems, we begin the continuation sequence with an initial penalty parameter of zero, $\gamma_1 = 0$, and set the initial design-variable values to $x_{ijk} = 1/K$, so that the linear constraints (5) are satisfied. We have found that for the optimization problems presented below, the continuation history and the optimal solution are insensitive to the starting point. We attribute this behavior to the setting of the initial penalty parameter to zero which eliminates the spherical constraints from the initial optimization problem. In this paper, we solve Opt($\gamma_n$) using the sequential quadratic optimization code SNOPT [Gill et al., 2005], through the Python-based wrapper in the optimization package pyOpt [Perez et al., 2012]. SNOPT is designed to satisfy all the linear constraints exactly at every iteration.

## 4 Adjacency constraints

Frequently the designer is not given complete freedom to choose a lamination sequence. Manufacturing requirements may place additional restrictions on the lamination sequence

that must be reflected in the optimization problem. To model some of these requirements, we introduce adjacency constraints, which impose limitations on the set of allowable ply angles in one layer based on the active ply-angle variable in an adjacent layer.

For the formulation of these constraints, consider the first layer, $j = 1$, of the design segments, $i = 1$ and $i = 2$, with design variables $x_{11k}$ and $x_{21p}$, respectively. If the design variable $x_{11k}$ is active at the solution, then the purpose of the adjacency constraint is to restrict the available choices in the adjacent layer to some reduced set of options. To formulate the adjacency constraint, we introduce sets of indices $\mathscr{I}_k$, for $k = 1,\ldots,K$, that represent the indices of the angles that *cannot* be used in an adjacent layer when the $k^{\text{th}}$-ply is active. Using these sets, the adjacency constraint can be imposed as follows:

$$\begin{aligned} x_{11k}x_{21p} \leq 0, \quad & k = 1,\ldots,K, \\ & p \in \mathscr{I}_k. \end{aligned} \tag{12}$$

This type of constraint, in combination with the condition $x_{ijk} \geq 0$, is a complementarity constraint, where the $\leq$ condition is used to conform to the standard complementarity constraint formulation. Unfortunately, complementarity constraints violate all conventional constraint qualifications such as the linear independence constraint qualification (LICQ) and the Mangasarian–Fromovitz constraint qualification (MFCQ) [Nocedal and Wright, 1999]. As a result, these types of constraints may not admit Lagrange multipliers at the solution, and gradient-based optimizers may encounter difficulties [Scheel and Scholtes, 2000, Scholtes, 2001].

Instead of using the complementarity constraint (12) directly, we use a regularization of the constraint due to Scholtes [2001]. In this regularization technique, the original complementarity constraint is perturbed in the following manner:

$$\begin{aligned} x_{11k}x_{21p} \leq \tau, \quad & k = 1,\ldots,K, \\ & p \in \mathscr{I}_k, \end{aligned} \tag{13}$$

for $\tau > 0$. A series of optimization problems is then solved for decreasing values of $\tau$ using a conventional SQP-based optimizer, with each new problem starting from the previous solution. This series of perturbed problems converges to a solution of the original problem with some conditions on the linear independence of the constraint gradients excluding the complementarity constraints [Scholtes, 2001].

There are many possible choices for the index sets, $\mathscr{I}_k$. We exclusively use a formulation in which the active ply-selection variable may shift by no more than $L$ indices between plies. In this case the index sets, $\mathscr{I}_k$ are defined as follows:

$$\mathscr{I}_k = \begin{cases} k \leq L & \{k+L+1,\ldots,K+k-L-1\} \\ k \geq K-L & \{k-K+L+1,\ldots,k-L-1\} \\ \text{otherwise} & \{1,2,\ldots,K\} \setminus \{k-L,\ldots,k+L\} \end{cases}. \tag{14}$$

The total number of adjacency constraints can be reduced by combining groups of the constraints (12) into a single equivalent constraint. Here, we use the equivalent constraint:

$$x_{11k} \sum_{p \in \mathscr{I}_k} x_{21p} \leq \tau, \quad k = 1,\ldots,K, \tag{15}$$

which produces one constraint per pair of constrained plies. For ease of presentation, we write all of the grouped adjacency constraints (15) in the following form:

$$\mathbf{d}(\mathbf{x}) \leq \tau, \tag{16}$$

where $\mathbf{d} \in \mathbb{R}^{n_a}$, where $n_a$ is the number of adjacency constraints in the form of Eq. (15).

Opt$'(\gamma, \tau)$, the original optimization problem (11) with the additional adjacency constraints, can be written as follows:

$$\begin{aligned} \min \quad & f(\mathbf{x}) + \gamma \mathbf{e}^T(\mathbf{e} - \mathbf{c}_s(\mathbf{x})) \\ \text{w.r.t.} \quad & \mathbf{x} \geq 0 \\ \text{s.t.} \quad & \mathbf{h}(\mathbf{x}) \geq 0 \\ & \mathbf{d}(\mathbf{x}) \leq \tau \\ & \mathbf{A}_w \mathbf{x} \equiv \mathbf{e} \end{aligned} \tag{17}$$

We solve the optimization problem Opt$'(\gamma_n, \tau_n)$ for a series $\{\gamma_n, \tau_n\}$ with nondecreasing $\gamma_n$ and nonincreasing $\tau_n$.

### 4.1 Using complementarity constraints to avoid intermediate designs

The penalization approach presented in Section 3 ensures that, for sufficiently large $\gamma$, solutions to the optimization problem with the full set of spherical constraints (8) are also solutions to the optimization problem (11). However, the converse is not true. That is, solutions of the modified $\ell_1$ penalty problem (11) may not be solutions to the original problem (8), even for large values of $\gamma$. Thus, for optimization problems with certain constraints, the sequence of solutions to Opt$(\gamma_n)$ may converge to a point at which $||\mathbf{c}_s(\mathbf{x}_n^*) - \mathbf{e}||_1 \neq 0$ even for large $\gamma_n$. These solutions are local minima since for a sufficiently large value of the penalty parameter, $\gamma_n$, any feasible 0–1 point, $\mathbf{x}_f$, with $||\mathbf{c}_s(\mathbf{x}_f) - \mathbf{e}||_1 = 0$, will have an objective value, $f(\mathbf{x}_f)$, lower than the penalized objective, $f(\mathbf{x}_n^*) + \gamma_n ||\mathbf{c}_s(\mathbf{x}_n^*) - \mathbf{e}||_1$, even if $f(\mathbf{x}_n^*) < f(\mathbf{x}_f)$.

We have found that Opt$(\gamma_n)$ may fail to converge to a 0–1 solution for problems in which additional constraints are imposed on the ply-selection variables. These additional constraints impose conditions such that any feasible path away from the local solution yields a higher value of the penalized objective. As a result, the continuation sequence does not move away from the intermediate design, and the solution does not proceed to a 0–1 point. To obtain a 0–1 solution in these cases we impose an additional constraint that forces the optimum away from the intermediate design. For each ply we add the following complementarity constraint:

$$\sum_{k=1}^{K-1} x_{ijk} \sum_{p=k+1}^{K} x_{ijp} \leq \tau, \quad i = 1, \ldots, M, \quad j = 1, \ldots, N.$$

This constraint ensures that as $\tau$ decreases, only a single ply-selection variable will be nonzero in each layer. However, by itself, this constraint does not force the design toward a 0–1 solution. We collect these constraints for each ply in every design segment into the following vector of constraints:

$$\mathbf{g}(\mathbf{x}) \leq \tau, \tag{18}$$

where $\mathbf{g}(\mathbf{x}) \in \mathbb{R}^{MN}$. As $\tau \to 0$, points at which more than one ply-selection variable is nonzero will become infeasible. While it would be possible to include this constraint for all optimization problems, we have found that optimization problems with constraint (18) tend to require more function and gradient evaluations. As a result, we include this complementarity constraint only when the infeasibility with respect to the spherical constraints $||\mathbf{c}_s(\mathbf{x}_n^*) - \mathbf{e}||_1$ is not reduced on subsequent continuation iterations for large values of the penalty parameter $\gamma_n$.

| Property | Value |
|---|---|
| $E_1$ | 54 GPa |
| $E_2$, $E_3$ | 18 GPa |
| $G_{12}$, $G_{13}$, $G_{23}$ | 9 GPa |
| $\nu_{12}$ | 0.25 |

Table 1: Material properties used for the single-layer plate compliance minimization problem

## 5 Compliance minimization studies

In this section, we present a series of compliance minimization problems for plates subject to pressure loading. These compliance minimization problems, which we denote by the generic label CompOpt$(\gamma, \tau)$, are formulated as follows:

$$\begin{aligned} \text{minimize} \quad & \alpha \frac{1}{2}\mathbf{u}^T\mathbf{K}\mathbf{u} + \gamma \mathbf{e}^T(\mathbf{e} - \mathbf{c}_s(\mathbf{x})) \\ \text{w.r.t.} \quad & \mathbf{x} \geq 0 \\ \text{governed by} \quad & \mathbf{K}\mathbf{u} = \mathbf{f} \\ \text{s.t.} \quad & \mathbf{d}(\mathbf{x}) \leq \tau \\ & \mathbf{A}_w\mathbf{x} \equiv \mathbf{e} \end{aligned} \tag{19}$$

where $\mathbf{u}$ are the nodal displacements, $\mathbf{K}$ is the stiffness matrix, $\mathbf{f}$ is the consistent force vector, and $\alpha$ is a scaling parameter that ensures that the compliance is scaled to a value close to unity. In all cases, the finite-element analysis is performed using the Toolkit for the Analysis of Composite Structures (TACS) [Kennedy and Martins, 2010], an advanced parallel finite-element code that includes an adjoint method for computing derivatives and has been successfully applied to aerostructural design optimization [Kennedy and Martins, 2012, Kenway et al., 2012].

For all the compliance cases, we do not use SIMP penalization and set $P = 1$. At each continuation iteration, we solve the optimization problem to an optimality and feasibility tolerance of $10^{-6}$. Each case presented here converges to a 0–1 solution such that the infeasibility of the spherical constraint $||\mathbf{c}_s(\mathbf{x}) - \mathbf{e}||_1$ is less than $10^{-10}$.

### 5.1 Single-layer plate

In this section, we give the results of our proposed laminate parametrization for Problems 9 and 10 presented by Hvejsel et al. [2011]. The objective of these problems is to obtain the ply-angle distribution in a fully clamped square plate with the dimensions $1\,\text{m} \times 1\,\text{m} \times 0.05\,\text{m}$, subject to a 100 kPa pressure load. The material properties associated with the plate are shown in Table 1. The plate is split into $20 \times 20$ design segments and the number of allowable ply angles is set to either $K = 4$ with $\Theta = \{0^\text{o}, \pm 45^\text{o}, 90^\text{o}\}$ or $K = 12$ with $\Theta = \{0^\text{o}, \pm 15^\text{o}, \pm 30^\text{o}, \pm 45^\text{o}, \pm 60^\text{o}, \pm 75^\text{o}, 90^\text{o}\}$. We use a finite-element model of the plate consisting of $20 \times 20$ third-order MITC9 shell elements, with just over 10 000 degrees of freedom. The design problem consists of 1600 design variables for the $K = 4$ case and 4800

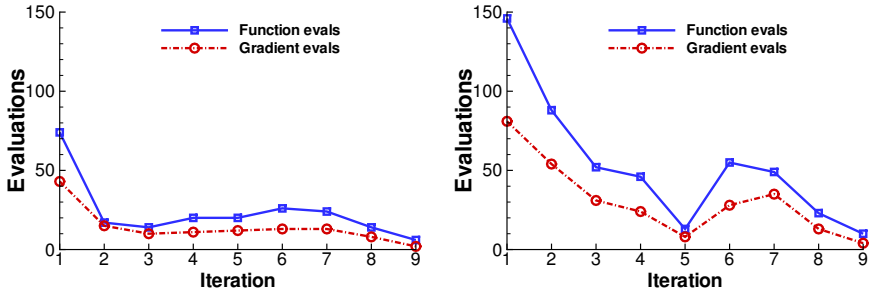


(a) Case $K = 4$ (b) Case $K = 12$

Fig. 2: Number of function and gradient evaluations as a function of the continuation history for the single-layer compliance minimization problem proposed by Hvejsel et al. [2011].

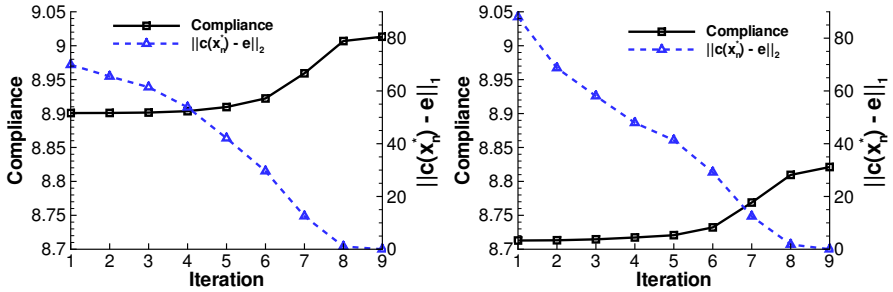


(a) Case $K = 4$ (b) Case $K = 12$

Fig. 3: Compliance and infeasibility in the spherical constraint as a function of the continuation history for the single-layer compliance minimization problem proposed by Hvejsel et al. [2011].

design variables for the $K = 12$ case. In both cases, we use the design problem formulation (19), without the adjacency constraints, and we set the parameter $\alpha = 1/9$ and use the sequence of parameters $\gamma_1 = 0$, $\gamma_n = 10^{-5}\,2^{n-2}$.

For the case $K = 4$, our approach requires 9 continuation iterations, with a total of 215 function evaluations and 127 gradient evaluations, and the final value of the compliance is 9.013 J. For the case $K = 12$, our approach requires 9 continuation iterations, with a total of 482 function evaluations and 278 gradient evaluations, and the final value of the compliance is 8.822 J. Figure 2 shows the number of function and gradient evaluations required to solve the optimization problem over the course of the continuation history. In both instances, the first optimization is the most costly, and the subsequent optimizations require fewer iterations. Overall, the optimization cost for $K = 12$ is far higher than the cost for $K = 4$.

Figure 3 shows the compliance and infeasibility of the spherical constraint as a function of the continuation history. In both cases the infeasibility decreases as the penalty parameter increases, and both of the final designs exhibit 0–1 solutions with $||\mathbf{c}_s(\mathbf{x}^*) - \mathbf{e}||_1 \leq 10^{-10}$.

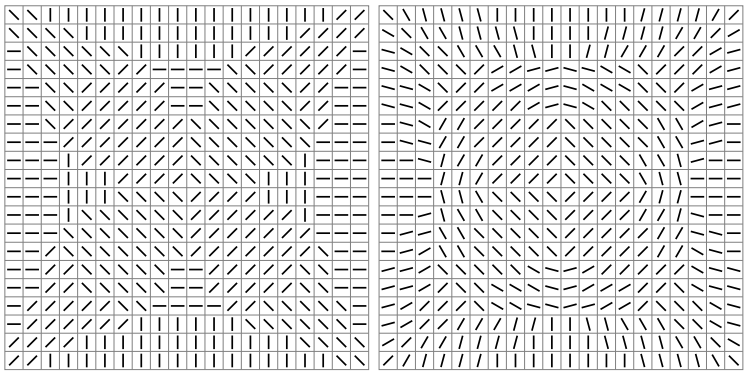

(a) Case $K = 4$ (b) Case $K = 12$

Fig. 4: Optimal ply angles for the single-layer compliance minimization problem proposed by Hvejsel et al. [2011].

| Property | Value |
|---|---|
| $E_{11}$ | 164 GPa |
| $E_{22}$ | 8.3 GPa |
| $G_{12}$, $G_{13}$ | 21.0 GPa |
| $G_{23}$ | 12 GPa |
| $\nu_{12}$ | 0.34 |
| $t_{\text{ply}}$ | 0.125 mm |

Table 2: Representative IM7/3501-6 stiffness and strength properties.

Figure 4 shows the optimal ply distributions for $K = 4$ and $K = 12$. For the $K = 4$ case, the ply distribution shown in Fig. 4a is identical to the result obtained by Hvejsel et al. [2011]. For the $K = 12$ case 16 plies have a discrepancy of $\pm 15^{\text{o}}$, representing only 4% of the plate. Overall the designs exhibit the same trends, with the ply angles creating concentric circles around the center of the plate, while the plies in the outer regions are pointed toward the center of the plate.

## 5.2 Eight-layer plate

In this section, we consider a fully clamped, 8-layer square plate subject to a surface pressure load. The plate is subdivided into $9 \times 9$ design segments, and the ply angles are restricted to $0^{\text{o}}$, $\pm 45^{\text{o}}$, and $90^{\text{o}}$ resulting in 4 ply-selection variables per design ply. Instead of designing all the angles independently, we link the plies in the middle four layers of the plate. We write this lamination sequence as $[C_1, C_2, \theta_3, \theta_4, \theta_5, \theta_6, C_7, C_8]$, where the design segments in the bottom layers, $C_1$, and $C_2$, and the top layers, $C_7$ and $C_8$, represent distributions of ply angles. The representative composite material properties used for this plate are listed in Table 2.

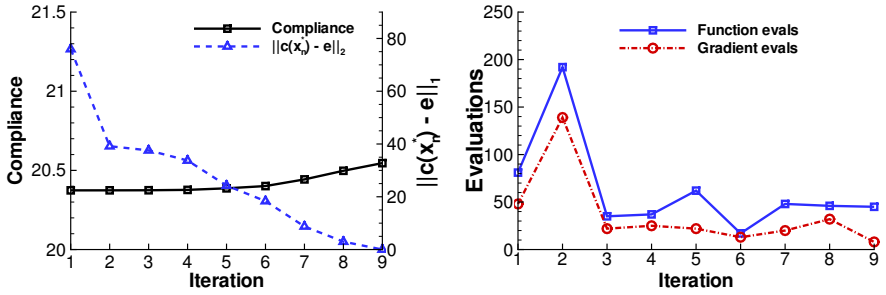


Fig. 5: Convergence history and function evaluations for the plate compliance problem with no adjacency constraints. Note that here the infeasibility is measured as $||\mathbf{c}_s(\mathbf{x}_n^*) - \mathbf{e}||_1$.

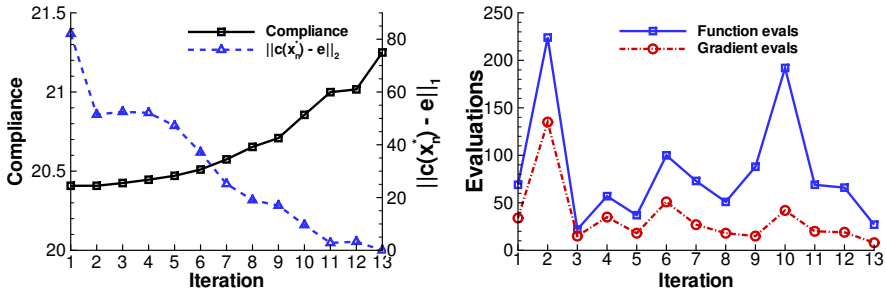


Fig. 6: Convergence history and function evaluations for the plate compliance problem with adjacency constraints. Note that here the infeasibility is measured as $||\mathbf{c}_s(\mathbf{x}_n^*) - \mathbf{e}||_1$.

The plate is $0.9\,\text{m} \times 0.9\,\text{m}$ and is subjected to a 1 kPa pressure such that the bottom layer of the laminate is in compression and the top layer of the laminate is in tension in the middle of the plate. The $9 \times 9$ design patches are modeled using $4 \times 4$ third-order MITC9 shell elements [Bathe and Dvorkin, 1986, Bucalem and Bathe, 1993]. The finite-element model contains 1296 elements, 5329 nodes, and just over 30 000 structural degrees of freedom. Here we use a scaling factor of $\alpha = 1/20$ to ensure that the scaled compliance function takes on values close to unity.

We solve this problem with and without the adjacency constraints introduced in Section 4. We use the formulation of the adjacency constraints (14), with $L = 1$ so that the ply angles are permitted to change by only $45^\text{o}$ between plies. We apply the adjacency constraints between the plies in adjoining design segments along the coordinate directions of the plate but not along the diagonal. This scheme results in a total of 576 adjacency constraints.

We solve a sequence of problems CompOpt$(\gamma_n, \tau_n)$, starting each new problem from the solution of the previous iteration. For the first iteration we select the penalty parameter $\gamma_1 = 0$, and for all subsequent iterations we take $\gamma_n = 2^{n-2}10^{-5}$ for $n \geq 2$, while for the regularization parameter, $\tau_n$, we use the sequence $\tau_n = 1/2(0.9)^{n-1}$.

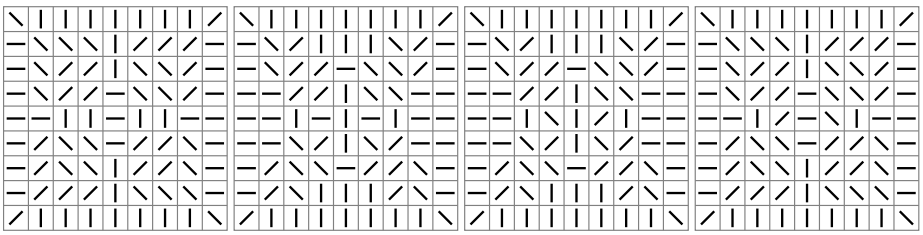

(a) Ply 1: $C_1$ (b) Ply 2: $C_2$ (c) Ply 7: $C_7$ (d) Ply 8: $C_8$

Fig. 7: Ply-angle distributions for the compliance minimization problem without the adjacency constraint.

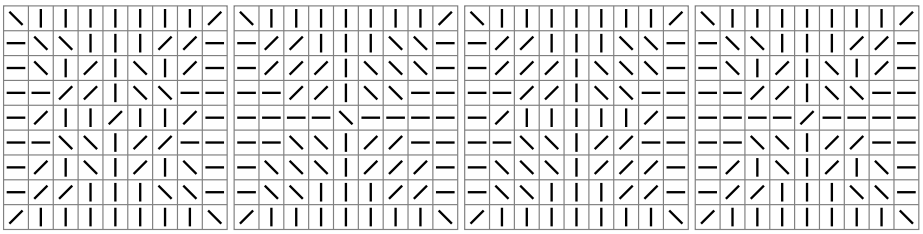

(a) Ply 1: $C_1$ (b) Ply 2: $C_2$ (c) Ply 7: $C_7$ (d) Ply 8: $C_8$

Fig. 8: Ply-angle distributions for the compliance minimization problem with the adjacency constraint.

Figure 5 shows the continuation convergence history and the function and gradient evaluations required to solve the compliance minimization problem without the adjacency constraints. The compliance minimization problem converges to a 0–1 point in 9 continuation iterations with a final compliance value of 20.545 J. The entire optimization requires a total of 563 function evaluations and 329 gradient evaluations. The main computational cost is incurred in the first two continuation iterations, while the remaining continuation optimizations are less expensive.

Figure 6 shows the convergence history and the function and gradient evaluations required to solve the compliance minimization problem with the adjacency constraints. The compliance problem with adjacency constraints requires 13 continuation iterations and converges to a 0–1 solution with a final compliance value of 21.250. The entire optimization process requires 1057 function evaluations and 437 gradient evaluations.

The compliance minimization problem without adjacency constraints converges to the design $[C_1, C_2, 0^o, 90^o, 90^o, 0^o, C_7, C_8]$ where the ply distributions $C_1$, $C_2$, $C_7$, and $C_8$ are shown in Fig. 7. The compliance minimization problem with adjacency constraints converges to the design $[C_1, C_2, 0^o, 90^o, 90^o, 0^o, C_7, C_8]$ where the ply distributions $C_1$, $C_2$, $C_7$, and $C_8$ are shown in Fig. 8. The two solutions share some similar characteristics: the center ply angles form roughly concentric circles, while the boundary plies are oriented toward the center of the plate. In both cases, the laminate is nonsymmetric through the thickness.

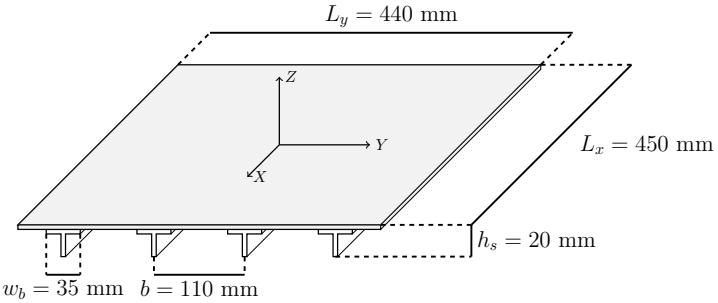


Fig. 9: Dimensions of the buckling optimization problem formulation.

## 6 Buckling optimization of a stiffened panel

In this section, we present the results from a series of optimizations of a stiffened panel with various design constraints. The geometry of the stiffened panel is shown in Fig. 9. The panel consists of four equally spaced stiffeners aligned along the $x$-direction. The panel is subjected to a prescribed end-shortening in the $x$-direction such that $u = -\Delta$ at $x = L_x$, and $u = 0$ at $x = 0$. The displacements along the $y = 0$ and $y = L_y$ edges of the skin are simply supported, while the stiffeners are permitted to elongate in the $z$-direction at the ends $x = 0$ and $x = L_x$. For this problem, we use the representative composite material data listed in Table 2.

We model the stiffened panel using a finite-element mesh consisting of 15 840 third-order MITC9 shell elements: 120 along the length, 128 in the transverse direction, and 5 through the depth of each stiffener. The finite-element model contains just over 383 000 degrees of freedom. We solve the linearized buckling eigenvalue problem on 16 processors using the parallel capabilities of TACS [Kennedy and Martins, 2010]. The buckling calculation consists of two steps. The first step is to determine the initial solution path $\mathbf{u}_p$ due to the forces caused by the prescribed end-shortening $\mathbf{f}_p$:

$$\mathbf{K}\mathbf{u}_p = \mathbf{f}_p.$$

Once the solution path $\mathbf{u}_p$ has been calculated, the second step is to solve the following linearized buckling eigenvalue analysis to determine the critical end-shortening, $\Delta_{cr}$, at the lowest buckling load:

$$\mathbf{K}\mathbf{u} + \Delta_{cr}\mathbf{G}(\mathbf{u}_p)\mathbf{u} = 0. \tag{20}$$

Here $\mathbf{G}(\mathbf{u}_p)$ is the geometric stiffness matrix, which is a function of the initial load path.

The sensitivities of the eigenvalues $d\Delta_{cr}/d\mathbf{x}$ can be determined if the derivatives of the stiffness matrix and the geometric stiffness matrices are known [Seyranian et al., 1994]. The most computationally expensive operation during the computation of $d\Delta_{cr}/d\mathbf{x}$ is the calculation of the derivative of the geometric stiffness matrix with respect to the design variables, which requires a contribution from the load-path computation. The derivative of

the geometric stiffness matrix can be found as follows:

$$\begin{aligned}\frac{d\mathbf{G}}{d\mathbf{x}} &= \frac{\partial \mathbf{G}}{\partial \mathbf{x}} + \frac{\partial \mathbf{G}}{\partial \mathbf{u}_p} \cdot \frac{d\mathbf{u}_p}{d\mathbf{x}}, \\ &= \frac{\partial \mathbf{G}}{\partial \mathbf{x}} + \frac{\partial \mathbf{G}}{\partial \mathbf{u}_p} \cdot \mathbf{K}^{-1} \frac{\partial}{\partial \mathbf{x}} \left[\mathbf{f}_p - \mathbf{K}\mathbf{u}_p\right],\end{aligned} \tag{21}$$

where the operator $(\cdot)$ is used to denote a tensor-vector inner product.

In this buckling problem, we assume that the geometry of the panel and the number of plies at $0^o$, $\pm 45^o$, and $90^o$ are fixed. This problem could arise during the buckling design of a stiffened panel where the stiffness and strength requirements dictate the geometry and ply content of the panel. The objective is to maximize the critical end-shortening of the panel by varying the lamination-stacking sequence subject to various constraints on the sequence of ply angles. Here, we fix the thicknesses of the skin, stiffener-base, and stiffener at 24, 30, and 20 plies respectively. The number of plies in the skin and the stiffener at $0^o$, $45^o$, $-45^o$, and $90^o$ are 8, 6, 6, and 4, and 10, 4, 4, and 2 respectively. The outer 6 plies on both sides of the stiffener form the bottom 6 plies of the stiffener pad. An additional 8 plies are added in the middle of the stiffener. Note that the laminates in the skin and stiffener are balanced, while the laminate of the stiffener-base may be nonsymmetric.

To obtain laminates with the prescribed number of plies, we impose the following linear constraint on the ply-selection variables:

$$\sum_{j=1}^{N} x_{ijk} = p_{ik}, \quad i = 1,\ldots,3, \quad k = 1,\ldots,4, \tag{22}$$

where $p_{ik}$ is the number of plies in component $i$ at ply angle $\theta_k$.

Matrix-cracking can occur in laminates when several contiguous plies are at the same angle [Haftka and Walsh, 1992]. To obtain laminate sequences that do not contain more than four repeated plies, we use the following complementarity constraint:

$$\prod_{j=p}^{p+5} x_{ijk} \leq \tau, \quad i = 1,\ldots,3 \quad p = 1,\ldots,N-5. \tag{23}$$

This constraint ensures that over a five-ply range, no more than four identical plies can be active.

We examine four different lamination-stacking sequence problems:

Case A Nonsymmetric skin, symmetric stiffener
Case B Symmetric skin and stiffener
Case C Nonsymmetric skin, symmetric stiffener, and no more than four contiguous plies at the same angle
Case D Symmetric skin and stiffener and no more than four contiguous plies at the same angle.

| | Case A | Case B | Case C | Case D |
|---|---|---|---|---|
| Design variables | | | | |
| Skin ply identity | 96 | 48 | 96 | 48 |
| Stiffener ply identity | 40 | 40 | 40 | 40 |
| Total | 136 | 88 | 136 | 88 |
| Constraints | | | | |
| Contiguity constraint ($\mathbf{c}_p(\mathbf{x}) \leq \tau$) | – | – | 120 | 88 |
| Local minima constraint ($\mathbf{g}(\mathbf{x}) \leq \tau$) | – | 22 | – | – |
| Ply content ($\mathbf{Bx} = \mathbf{p}$) | 8 | 8 | 8 | 8 |
| Linear weights ($\mathbf{A}_w\mathbf{x} \equiv \mathbf{e}$) | 34 | 22 | 34 | 22 |
| Total | 42 | 52 | 162 | 118 |

Table 3: Design problem summary for the buckling optimization studies

Each of these optimization problems can be expressed via the following formulation, which we denote BucklingOpt$(\gamma, \tau)$:

$$\begin{aligned} \text{maximize} \quad & \Delta_{cr} - \gamma \mathbf{e}^T(\mathbf{e} - \mathbf{c}_s(\mathbf{x})) \\ \text{w.r.t.} \quad & \mathbf{x} \geq 0 \\ \text{governed by} \quad & \mathbf{K}\mathbf{u}_p = \mathbf{f}_p \\ & \mathbf{K}\mathbf{u} + \Delta_{cr}\mathbf{G}(\mathbf{u}_p)\mathbf{u} = 0 \\ \text{s.t.} \quad & \mathbf{c}_p(\mathbf{x}) \leq \tau \\ & \mathbf{g}(\mathbf{x}) \leq \tau \\ & \mathbf{Bx} = \mathbf{p} \\ & \mathbf{A}_w\mathbf{x} \equiv \mathbf{e} \end{aligned} \tag{24}$$

where $\mathbf{Bx} = \mathbf{p}$ are the ply constraints (22) and $\mathbf{c}_p(\mathbf{x}) \leq \tau$ are the contiguous ply constraints (23). Table 3 summarizes the design problems for the four buckling optimization cases. Note that for Case B we have added the complementarity constraints, $\mathbf{g}(\mathbf{x}) \leq \tau$, from Eq. (18) to avoid local minima with intermediate designs. We have found that, because of symmetry and the ply-content constraints, the $\pm 45^{\text{o}}$ layers converge to a local minimum with equal weights of $1/2$. Without this additional constraint, Case B does not converge to a 0–1 point, even for large $\gamma$.

For all the cases, we use a sequence of penalty parameters $\gamma_1 = 0$, $\gamma_n = 2^{n-2}10^{-5}$ for $n \geq 2$ and a regularization parameter sequence of $\tau_n = (1/2)(0.9)^{n-1}$.

The lamination sequences for all cases are shown in Fig. 10, for the skin, stiffener-base, and stiffener laminates respectively. The nonsymmetric skin design, Case A, converges to a slightly better result than the symmetric skin design, Case B. Likewise, the nonsymmetric skin design with ply-contiguity constraints, Case C, converges to a slightly better design than the symmetric skin design with ply-contiguity constraints, Case D. In both the symmetric and nonsymmetric designs, the redistribution of the ply angles results in about a 1% reduction in the critical end-shortening.

For the skin layup of both Case A and Case B, the $0^{\text{o}}$ plies are placed in the middle, the $90^{\text{o}}$ plies are placed on the exterior, and the $\pm 45^{\text{o}}$ plies are placed in between. The difference between Case A and Case B is that for Case A the $0^{\text{o}}$ plies are offset from the middle and the

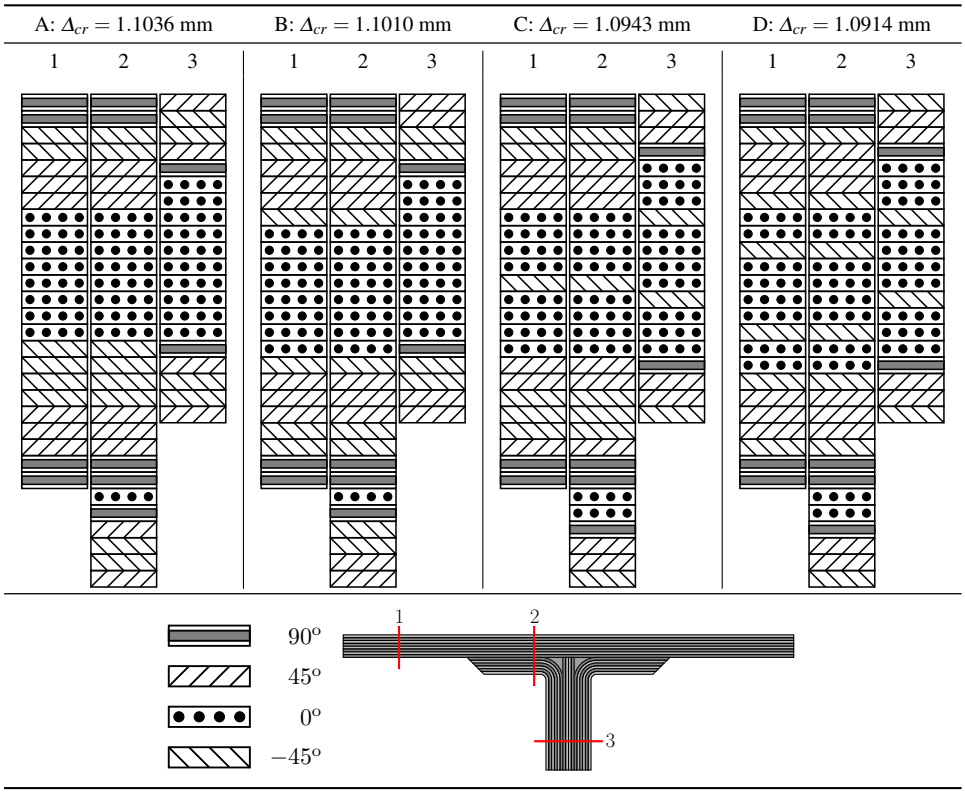


Fig. 10: Optimal ply-angle sequences for the buckling optimization problems. Each solution shows the skin, stiffener-base, and skin layups, respectively.

arrangement of the $\pm 45^{\circ}$ plies is altered. This arrangement of ply angles is used to suppress the overall buckling mode that involves both the skin and stiffeners.

Case C and Case D converge to solutions similar to those for Cases A and B. However, the ply-contiguity constraint forces Cases C and D to include additional $-45^{\circ}$ plies in the middle of the stiffener and skin to break up the large segment of $0^{\circ}$ plies in the original designs. These requirements have a small negative impact on the buckling performance.

Figure 11 shows the continuation history of the objective for all the cases. They all converge to a 0–1 design within 10 to 14 continuation iterations. Cases A and C and Cases B and D arrive at the same design after the first continuation iteration. For Cases C and D, with the ply-contiguity constraints, the objective drops significantly between the first and second continuation iterations, while for Cases A and B, without the ply-contiguity constraints, the objective decreases only near the end of the continuation iterations. Note that only the final objective value represents a physically realizable laminate. All prior continuation iterations represent intermediate designs.

Figure 12 shows the continuation history of the infeasibility of the spherical constraints, as measured by $||\mathbf{c}_s(\mathbf{x}) - \mathbf{e}||_1$. Note that the infeasibility falls below $10^{-10}$ on the final iteration for all cases. The infeasibility for Cases A and B does not change between the first and

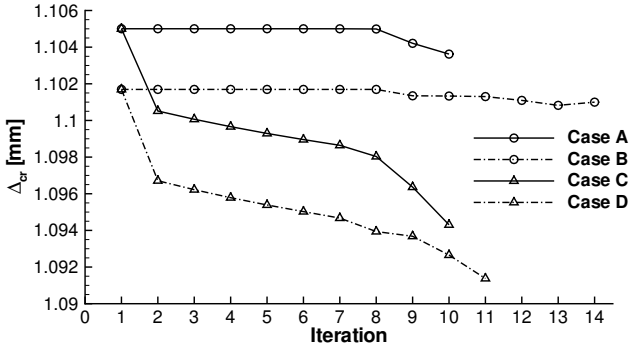


Fig. 11: Convergence of the objective $\Delta_{cr}$, for Cases A, B, C, and D.

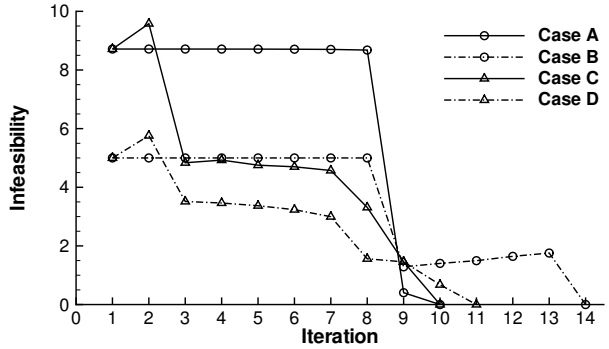


Fig. 12: Convergence of the infeasibility as measured by $||\mathbf{c}_s(\mathbf{x}_n^*) - \mathbf{e}||_1$ for Cases A, B, C, and D.

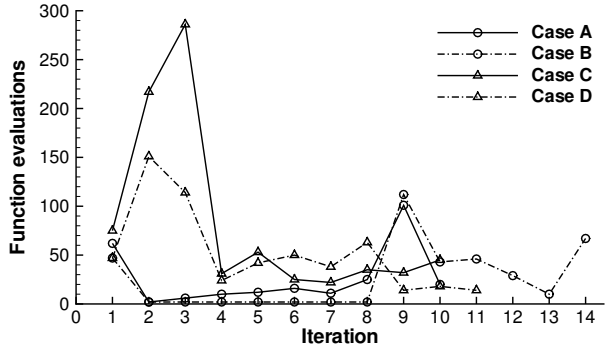


Fig. 13: Number of function evaluations for the continuation iterations for Cases A, B, C, and D.

eighth iterations, and then it decreases rapidly in both cases. The infeasibility for Cases C and D decreases more slowly; this behavior is due, in part, to the ply-contiguity constraints.

Figure 13 shows the number of function evaluations required for each continuation iteration for all the cases. The number of gradient evaluations and the overall optimization cost is approximately proportional to the number of function evaluations and is not shown here. Case A requires a total of 265 function evaluations and 72 gradient evaluations, Case B requires a total of 368 function evaluations and 94 gradient evaluations, Case C requires a total of 821 function evaluations and 218 gradient evaluations, and Case D requires a total of 575 function evaluations and 127 gradient evaluations. Clearly the optimizations for Cases C and D require significantly more function and gradient evaluations than do those for Cases A and B, where the main additional cost is incurred in the first three continuation steps. On the other hand, Cases A and B are less computationally expensive and require far fewer function and gradient evaluations.

## 7 Conclusions

In this paper, we have presented a novel laminate parametrization technique that can be used to determine the laminate-stacking sequence of a layered composite structure. In this approach, the laminate stiffness is expressed in terms of ply-selection variables. Instead of using discrete variables in the optimization problem, which leads to a nonlinear mixed-integer formulation, we use a continuous relaxation of the discrete problem and impose an additional spherical constraint so that the solution to the continuous problem satisfies the 0–1 criterion. Instead of introducing these constraints directly into the problem, we add them through an exact $\ell_1$-penalty function so that the solutions to the relaxed problem are also solutions to the penalized problem, for sufficiently large values of the penalty parameter $\gamma$. Additional simplifications can be achieved if the linear constraints on the ply-identity variables are satisfied exactly at every iteration in the optimization problem. This approach can be used as an independent penalization or as an additional penalization for discrete material optimization (DMO) parametrizations that use a SIMP approach.

We have applied the proposed parametrization technique to both compliance minimization and buckling design problems with up to 4800 design variables. We presented a comparision of our method with the approach presented by Hvejsel et al. [2011]; we demonstrated exact agreement for one problem and only small discrepancies for a second problem. We then applied our parametrization to the design of an eight-ply laminate with and without adjacency constraints. Finally, we applied the parametrization to the design of a laminated stiffened panel for buckling. The results demonstrate that our parametrization method can be applied effectively to both compliance and buckling design problems. Future work will be devoted to incorporating strength-based design criteria into the parametrization.

## Acknowledgement

The computations for this paper were performed on the GPC supercomputer at the SciNet HPC Consortium at the University of Toronto. SciNet is funded by the Canada Foundation for Innovation, under the auspices of Compute Canada, the Government of Ontario, and the University of Toronto.

## References


D. B. Adams, L. T. Watson, Z. Gurdal, and C. M. Anderson-Cook. Genetic algorithm optimization and blending of composite laminates by locally reducing laminate thickness. *Advances in Engineering Software*, 35(1):35 – 43, 2004. ISSN 0965-9978. doi:10.1016/j.advengsoft.2003.09.001.

K.-J. Bathe and E. N. Dvorkin. A formulation of general shell elements the use of mixed interpolation of tensorial components. *International Journal for Numerical Methods in Engineering*, 22:697–722, 1986. ISSN 1097-0207. doi:10.1002/nme.1620220312.

T. Borrvall and J. Petersson. Topology optimization using regularized intermediate density control. *Computer Methods in Applied Mechanics and Engineering*, 190(3738):4911 – 4928, 2001. ISSN 0045-7825. doi:10.1016/S0045-7825(00)00356-X.

M. Bruyneel. A general and effective approach for the optimal design of fiber reinforced composite structures. *Composites Science and Technology*, 66(10):1303 – 1314, 2006. ISSN 0266-3538. doi:10.1016/j.compscitech.2005.10.011.

M. Bruyneel. SFP - A new parameterization based on shape functions for optimal material selection: application to conventional composite plies. *Structural and Multidisciplinary Optimization*, 43:17–27, 2011. ISSN 1615-147X. doi:10.1007/s00158-010-0548-0.

M. Bruyneel and C. Fleury. Composite structures optimization using sequential convex programming. *Advances in Engineering Software*, 33(7-10):697 – 711, 2002. ISSN 0965-9978. doi:10.1016/S0965-9978(02)00053-4.

M. Bruyneel, P. Duysinx, C. Fleury, and T. Gao. Extensions of the shape functions with penalization parametrization for composite-ply optimization. *AIAA Journal*, 49(10):2325–2329, October 2011. doi:10.2514/1.J051225.

M. L. Bucalem and K.-J. Bathe. Higher-order MITC general shell elements. *International Journal for Numerical Methods in Engineering*, 36:3729–3754, 1993. ISSN 1097-0207. doi:10.1002/nme.1620362109.

J. Foldager, J. S. Hansen, and N. Olhoff. A general approach forcing convexity of ply angle optimization in composite laminates. *Structural and Multidisciplinary Optimization*, 16: 201–211, 1998. ISSN 1615-147X. doi:10.1007/BF01202831.

H. Fukunaga and H. Sekine. Stiffness design method of symmetric laminates using lamination parameters. *AIAA Journal*, 30(11):2791–2793, 1992.

H. Fukunaga and G. N. Vanderplaats. Stiffness optimization of othrotropic laminated composites using lamination parameters. *AIAA Journal*, 29(4):641–646, 1991.

T. Gao, W. Zhang, and P. Duysinx. A bi-value coding parameterization scheme for the discrete optimal orientation design of the composite laminate. *International Journal for Numerical Methods in Engineering*, 91(1):98–114, 2012. ISSN 1097-0207. doi:10.1002/nme.4270.

P. E. Gill, W. Murray, and M. A. Saunders. SNOPT: An SQP algorithm for large-scale constrained optimization. *SIAM Review*, 47(1):pp. 99–131, 2005. ISSN 00361445.

R. Haftka and Z. Gürdal. *Elements of Structural Optimization*. Solid mechanics and its applications. Kluwer Academic Publishers, 1992. ISBN 9780792315049.

R. T. Haftka and J. L. Walsh. Stacking-sequence optimization for buckling of laminated plates by integer programming. *AIAA Journal*, 30(3):814–819, March 1992.

V. B. Hammer, M. P. Bendse, R. Lipton, and P. Pedersen. Parametrization in laminate design for optimal compliance. *International Journal of Solids and Structures*, 34(4):415 – 434, 1997. ISSN 0020-7683. doi:10.1016/S0020-7683(96)00023-6.

C. Hvejsel and E. Lund. Material interpolation schemes for unified topology and multi-material optimization. *Structural and Multidisciplinary Optimization*, 43:811–825, 2011.

ISSN 1615-147X. 10.1007/s00158-011-0625-z.

C. Hvejsel, E. Lund, and M. Stolpe. Optimization strategies for discrete multi-material stiffness optimization. *Structural and Multidisciplinary Optimization*, 44:149–163, 2011. ISSN 1615-147X. doi:10.1007/s00158-011-0648-5.

S. T. IJsselmuiden, M. M. Abdalla, and Z. Gurdal. Implementation of strength-based failure criteria in the lamination parameter design space. *AIAA Journal*, 46(7):1826–1834, July 2008. doi:10.2514/1.35565.

K. A. James, J. S. Hansen, and J. R. R. A. Martins. Structural topology optimization for multiple load cases while avoiding local minima. In *Proceedings of the 4th AIAA Multidisciplinary Design Optimization Specialist Conference*, Schaumburg, IL, April 2008. AIAA 2008-2287.

K. A. James, J. S. Hansen, and J. R. R. A. Martins. Structural topology optimization for multiple load cases using a dynamic aggregation technique. *Engineering Optimization*, 41(12):1103–1118, December 2009. doi:10.1080/03052150902926827.

R. M. Jones. *Mechanics of Composite Materials*. Technomic Publishing Co., 1996.

G. J. Kennedy and J. R. R. A. Martins. Parallel solution methods for aerostructural analysis and design optimization. In *Proceedings of the 13th AIAA/ISSMO Multidisciplinary Analysis Optimization Conference*, Fort Worth, TX, September 2010. AIAA 2010-9308.

G. J. Kennedy and J. R. R. A. Martins. A comparison of metallic and composite aircraft wings using aerostructural design optimization. In *14th AIAA/ISSMO Multidisciplinary Analysis and Optimization Conference*, Indianapolis, IN, September 2012.

G. K. W. Kenway, G. J. Kennedy, and J. R. R. A. Martins. A scalable parallel approach for high-fidelity aerostructural analysis and sensitivity analysis. *AIAA Journal*, August 2012. Submitted for review, Manuscript id: 2012-08-J052255.

R. Le Riche and R. T. Haftka. Optimization of laminate stacking sequence for buckling load maximization by genetic algorithm. *AIAA Journal*, 31(5):951–956, May 1993.

B. Liu, R. T. Haftka, M. A. Akgn, and A. Todoroki. Permutation genetic algorithm for stacking sequence design of composite laminates. *Computer Methods in Applied Mechanics and Engineering*, 186(24):357 – 372, 2000. ISSN 0045-7825. doi:10.1016/S0045-7825(99)90391-2.

B. Liu, R. T. Haftka, and P. Trompette. Maximization of buckling loads of composite panels using flexural lamination parameters. *Structural and Multidisciplinary Optimization*, 26: 28–36, 2004. ISSN 1615-147X. doi:10.1007/s00158-003-0314-7.

E. Lund. Buckling topology optimization of laminated multi-material composite shell structures. *Composite Structures*, 91(2):158 – 167, 2009. ISSN 0263-8223. doi:10.1016/j.compstruct.2009.04.046.

M. Miki and Y. Sugiyama. Optimum design of laminated composites plates using lamination parameters. *AIAA Journal*, 31(5):921–922, 1993.

J. Nocedal and S. J. Wright. *Numerical Optimization*. Springer, 1999.

R. E. Perez, P. W. Jansen, and J. R. R. A. Martins. pyOpt: a Python-based object-oriented framework for nonlinear constrained optimization. *Structural and Multidisciplinary Optimization*, 45(1):101–118, 2012. doi:10.1007/s00158-011-0666-3.

H. Scheel and S. Scholtes. Mathematical programs with complementarity constraints: Stationarity, optimality, and sensitivity. *Mathematics of Operations Research*, 25(1):pp. 1–22, 2000. ISSN 0364765X.

S. Scholtes. Convergence properties of a regularization scheme for mathematical programs with complementarity constraints. *SIAM Journal on Optimization*, 11(4):918–936, 2001. ISSN 10526234. doi:10.1137/S1052623499361233.

A. P. Seyranian, E. Lund, and N. Olhoff. Multiple eigenvalues in structural optimization problems. *Structural and Multidisciplinary Optimization*, 8:207–227, 1994. ISSN 1615-147X. doi:10.1007/BF01742705.

O. Sigmund and S. Torquato. Design of materials with extreme thermal expansion using a three-phase topology optimization method. *Journal of the Mechanics and Physics of Solids*, 45(6):1037 – 1067, 1997. ISSN 0022-5096. doi:10.1016/S0022-5096(96)00114-7.

J. Stegmann and E. Lund. Discrete material optimization of general composite shell structures. *International Journal for Numerical Methods in Engineering*, pages 2009–2027, 2005. ISSN 1097-0207. doi:10.1002/nme.1259.

M. Stolpe and K. Svanberg. On the trajectories of the epsilon-relaxation approach for stress-constrained truss topology optimization. *Structural and Multidisciplinary Optimization*, 21:140–151, 2001a. ISSN 1615-147X. doi:10.1007/s001580050178.

M. Stolpe and K. Svanberg. On the trajectories of penalization methods for topology optimization. *Structural and Multidisciplinary Optimization*, 21:128–139, 2001b. ISSN 1615-147X. doi:10.1007/s001580050177.

S. W. Tsai and N. J. Pagano. Invariant properties of composite materials. In S. W. Tsai, editor, *Composite materials workshop, Vol. 1 of Progress in material science*, pages 233–253. Technomic Publishing Co., 1968.